GaInNAsSb for 1.3–1.6-μm-Long Wavelength Lasers Grown by Molecular Beam Epitaxy

Vincent Gambin, Wonill Ha, Mark Wistey, Homan Yuen, Seth R. Bank, Seongsin M. Kim, and James S. Harris, Jr., *Fellow, IEEE*

***Abstract*—High-efficiency optical emission past 1.3 μm of GaInNAs on GaAs, with an ultimate goal of a high-power 1.55-μm vertical-cavity surface-emitting laser (VCSEL), has proven to be elusive. While GaInNAs could theoretically be grown lattice-matched to GaAs with a very small bandgap [1], wavelengths are actually limited by the N solubility limit and the high In strain limit. By adding Sb to the GaInNAs quaternary, we have observed a remarkable shift toward longer luminescent wavelengths while maintaining high intensity. The increase in strain of these new alloys necessitates the use of tensile strain compensating GaNAs barriers around quantum-well (QW) structures. With the incorporation of Sb and using In concentrations as high as 40%, high-intensity photoluminescence (PL) was observed as long as 1.6 μm. PL at 1.5 μm was measured with peak intensity over 50% of the best 1.3 μm GaInNAs samples grown. Three QW GaInNAsSb in-plane lasers were fabricated with room-temperature pulsed operation out to 1.49 μm.**

***Index Terms*—Antimony compounds, GaInNAs, GaInNAsSb, gallium compounds, GaNAs, molecular beam epitaxy, nitrogen compounds, optical fiber communications, optical fiber lasers, PL, Raman amplifier, RBS, semiconductor lasers, SIMS, surfactant, VCSEL.**

I. Introduction

ALLOYS of GaInNAs have recently been studied in great detail for their application in long wavelength lasers and optical devices grown on GaAs. Wavelengths between 1.3 and 1.6 μm are of primary importance in optical local area networks (LANs) and metro area networks (MANs) and long-haul communications due to the low dispersion and minimum loss in optical fiber. The requirements for these optical communication lasers are single mode operation, a broad operating temperature range (-10 °C–90 °C), emission spectra over 1.3–1.6 μm, and moderate power (>10 mW). There is also significant interest in higher power pump lasers for Raman amplifiers to greatly increase the available bandwidth in existing fiber systems. InP-based lasers have serious fundamental shortcomings that hinder their ability to cover this wavelength range [2], both for low-cost vertical-cavity surface-emitting lasers (VCSELs) and high-power Raman pumps.

Much research has now been done showing that GaInNAs, that is coherently lattice-matched to GaAs [3]–[5], can have a bandgap energy in the wavelength range of 1.3 to 1.55 μm, and have properties which would fulfill the requirements of optical communication systems [1]. However, solid solubility of nitrogen in GaAs only exists for concentrations of less than about 5%. Wavelengths are then ultimately limited by the amount of In which can be added while remaining below the critical thickness for dislocation formation. High photoluminescence (PL) efficiency GaInNAs material has been grown that extends out to 1.3 μm, but beyond that wavelength, material quality commonly degrades rather seriously. Lasers utilizing these longer wavelength active materials exhibit extremely high threshold current densities and lower output power [6].

In this paper, two techniques were investigated to expand the feasible emission wavelengths for this material system. First, Sb present during GaInNAs growth has been thought to act only as a surfactant to improve quantum-well (QW) planarity and PL [7], [8]. With the addition of Sb, we have observed a sharp increase in radiative recombination with high In samples past 1.3 μm and found it not only acts as a surfactant, but is a significant alloy constituent, further red-shifting the optical emission. Second, tensile-strained GaNAs barriers between highly compressive GaInNAs QWs can be designed for strain compensation and can further red-shift output by reducing confinement energy in QWs. Since Sb in GaAs is compressively strained, there is further need for GaNAs strain compensating barriers, particularly in high-power devices where increasing the volume of the gain medium increases power output.

II. Material Growth and Testing

All samples were grown by solid source molecular beam epitaxy (MBE) with thermally cracked arsenic and antimony. Nitrogen was added using a radio-frequency (RF) plasma source. For all growths, the nitrogen flow rate was fixed at 0.5 sccm and RF power was 300 W. Due to the difficulty in calibrating the composition of five component systems with mixed group V components, such as GaInNAsSb, only the Sb beam flux, not growth rate, was recorded during growth. Indium and nitrogen content were calibrated using high-resolution X-ray diffraction (HRXRD) of GaInAs and GaNAs thin films. In order to change the nitrogen concentration, plasma conditions remained fixed while group III growth rate was varied, linearly changing the nitrogen incorporation. During nitride-arsenide growth, substrate temperatures were kept low, around 420 °C, in order to enhance N solid solubility. Only at low growth temperatures is phase segregation avoided, maintaining good surface morphology and high luminescent efficiency.

Manuscript received April 2, 2002; revised May 8, 2002. This work was supported in part by the Optoelectronics Materials Center under Contract MDA972-94-1-0003, Contract MDA972-98-1-0002, and Contract MDA972-00-1-0024; in part by DARPA/ARO under Contract DAAG55-98-1-0437; and in part by ONR under Contract N00014-01-1-0010.

The authors are with Stanford University, Stanford, CA 94305 USA (e-mail: vgambin@stanford.edu).

Digital Object Identifier 10.1109/JSTQE.2002.800843.

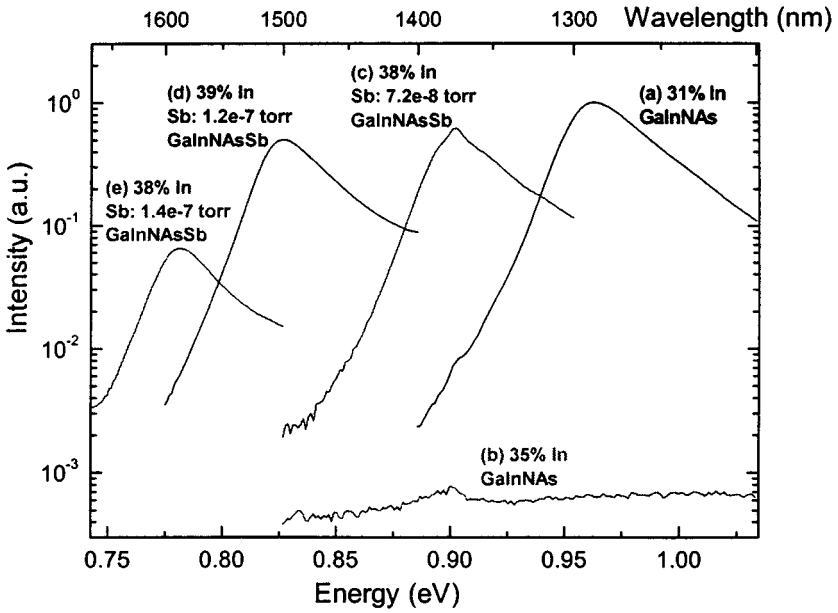

Fig. 1. Background subtracted PL results from two GaInNAs–GaNAs samples and three GaInNAsSb–GaNAsSb single QW samples. Nitrogen content remained fixed at 1.2%. Only Sb beam flux was measured in samples (c)–(d), while N and In were calibrated using HRXRD and RBS.

Samples underwent postgrowth rapid thermal anneal (RTA) in order to improve optical output of as-grown material. RTA was done under nitrogen ambient using GaAs as a proximity cap. Annealing temperatures were optimized for each sample due to a changing ideal thermal treatment for differing growth conditions and compositions. Laser samples were annealed at lower temperatures than PL samples due to the increased thermal exposure during cladding or mirror growth.

All PL samples measured were excited with a 514-nm Ar+ laser with 280 mW of incident power. In all spectra acquired, the system response was measured and removed from the PL measurement in order to compare signals over wide wavelength ranges. The resulting luminescence was detected using an uncooled GaInAs photodiode with standard lock-in techniques. In-plane lasers were mounted on a temperature-controlled copper block for characterization measurements. Light output was measured using a calibrated broad area GaInAs photodiode and spectral data was obtained by coupling into an optical spectrum analyzer (OSA).

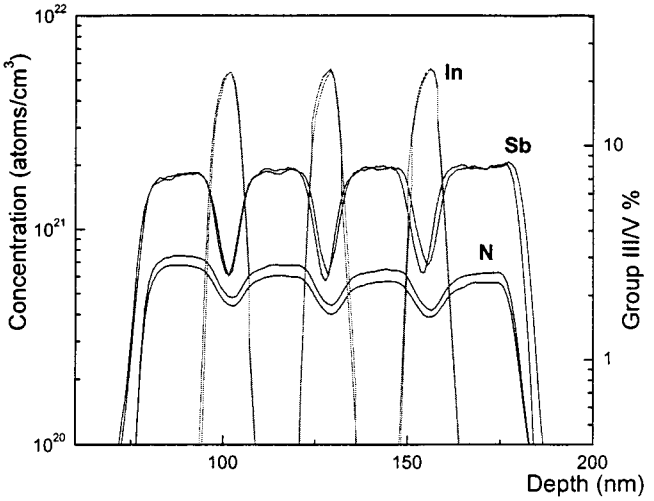

Fig. 2. SIMS profile of In, Sb, and N before and after RTA. The structure consisted of three GaInNAsSb QWs between GaNAsSb barriers. In and Sb profiles were not found to be significantly changed by the thermal process while annealing reduced the nitrogen concentration in barrier and QW.

III. Results and Discussion

A comparison of the brightest single QW GaInNAs and GaInNAsSb samples of increasing PL wavelength is shown in Fig. 1. Sample (a) in Fig. 1 is the highest intensity 1.3-μm PL sample grown thus far and consisted of 1.2% N and 31% In. Simply adding 4% In with the same N content, as shown in sample (b), red-shifts the optical output but has a tremendously deleterious effect on intensity, dropping by more than three orders of magnitude. However in sample (c), by keeping the N content at 1.2% and adding small amounts of Sb, the PL output shifted to 1.38 μm with little loss of efficiency. Increasing the Sb flux further during growth in sample (d), red-shifted PL to 1.5 μm with peak emission still over 50% that of the best 1.3-μm sample. Finally, an additional increase in Sb flux took wavelengths to 1.58 μm with only a further small reduction in output peak intensity.

Fig. 2 shows the In, N, and Sb secondary ion mass spectrometry (SIMS) profiles of a typical three-QW PL sample before and after annealing. All elements were calibrated using Rutherford backscattering spectrometry (RBS) with a GaInNAsSb standard thin film sample. Nitrogen was quantified using nuclear reaction analysis (NRA) RBS in which He++ ions of resonant energies induce a nuclear reaction in nitrogen [9]. This nuclear reaction subsequently releases protons of characteristic energies and quantitative chemical composition can be obtained with parts per million (ppm) accuracy. Due to the similar collision cross-sectional areas, standard RBS cannot accurately distinguish between In and Sb. Therefore, calibration of Sb was done with particle-induced X-ray emission (PIXE) RBS. In the PIXE measurement, characteristic X-rays from target elements are acquired during charge particle beam excitation in order

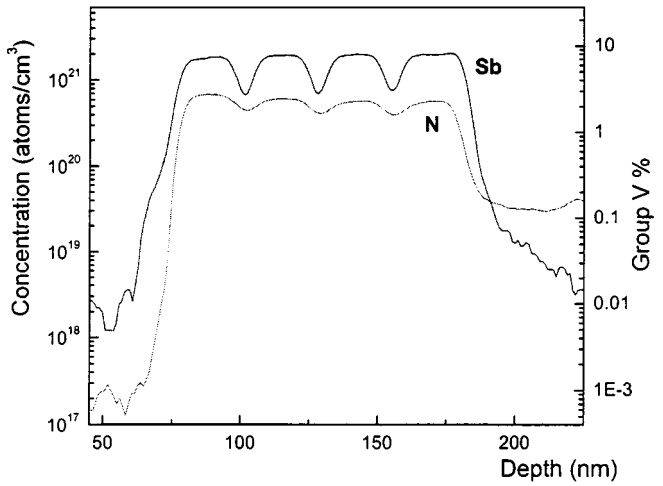

Fig. 3. Expanded view of Fig. 2 Sb and N SIMS profiles. All concentrations were calibrated with RBS techniques using calibration standards and calculated using an RBS measured GaInNAsSb density of 4.94 atoms/cm^3.

TABLE I
RESULTS FROM NRA-RBS AND PIXE-RBS OF GaInNAsSb CALIBRATION THIN FILM SAMPLES*

Sample	%N	Interstitial %
GaInNAs (8%In)	2.4	3.7
- Annealed	2.4	4.2
GaInNAsSb (8%In 7%Sb)	3.0	6.9
- Annealed	3.0	8.2
GaNAs (modified)	3	26
- Annealed (modified)	3	16

*Samples denoted as modified were grown at half the N_2 flow rate and with a larger aperture between plasma and substrate. The loss of nitrogen due to anneal is below the statistical measurement error for RBS and more difficult to measure in these thicker calibration samples.

to quantify chemical composition. The SIMS sample in Fig. 2 was a three-QW GaInNAsSb of 7 nm with 20-nm GaNAsSb barriers. A flux of 7.8×10^{-8} torr of cracked Sb was used during both QW and barrier growth. Before annealing, weak peak PL emission was found at 1.44 μm and after an RTA of 820 °C for 1 min peak emission was at 1.32 μm with 50 times higher intensity. As seen in the profiles, the only significant change in composition is the loss of nitrogen after annealing. The last QW and barrier do not precisely overlap in the Sb SIMS profile, but this is probably due to misadjusted sputter rates for that measurement run.

No Sb segregation during growth has been observed in the active region, as shown in Fig. 3. Antimony incorporates as high as 8% in the barriers where the growth rate is the slowest and 2.5% in the QWs during faster growth rates. Nitrogen behaves similarly, incorporating in the barriers higher then the QWs due to their increased growth rate. The N incorporated ideally with concentration varying proportionally with the inverse of the group III flux. However, the Sb composition between the QW and barrier does not follow a linear dependence on the growth rate and the composition in the QW is 54% less than what would be expected based on growth rate changes alone. This indicates that either the Sb incorporation has a nonlinear inverse growth rate dependence, changes with strain, or is highly dependent on the group III components. Further studies are currently being done to investigate this phenomenon in greater detail.

Common defects, such as interstitials, can cause misinterpretation of SIMS results. This is particularly important in nitride based material grown with high-energy techniques, such as RF plasma deposition, where accelerated ions or "hot" neutrals can impact the substrate, damaging the crystal or even implanting as a defect. All the material thus far analyzed by SIMS had interstitial concentrations below 7% measured using the difference between a channeled and random orientation in NRA-RBS as shown in Table I. In fact, interstitial concentration actually increased by 1%–3% on annealing most likely during RTA treatment under nitrogen ambient. However, this low concentration

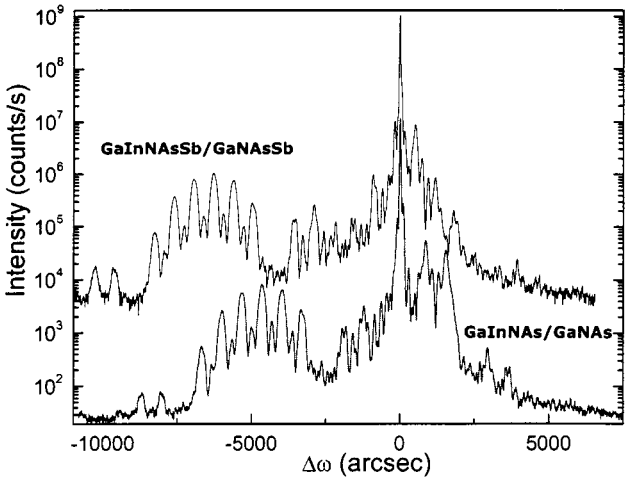

Fig. 4. HRXRD (004) rocking scan of GaInNAsSb–GaNAsSb and GaInNAs–GaNAs three-QW structures of 7 nm with 20-nm barriers. Scans were taken using a hybrid X-ray mirror and two crystal Ge (220) four-bounce monochromator with Cu Kα_2 radiation.

of interstitials was only obtained after modifying the nitrogen plasma growth conditions. With lower nitrogen flow rates and a larger aperture between plasma and substrate, the interstitial concentration was as high as 26% [9]. Finally, we also found that in the presence of Sb, the nitrogen content increased. Under identical growth rates and plasma conditions, the nitrogen content increased from 2.4% to 3.0% with the addition of Sb as measured with NRA-RBS. This small increase in nitrogen, while interesting, does not alone account for the large bandgap reduction observed by adding Sb to GaInNAs.

The amount of compressive strain present in the high indium GaInNAsSb QW samples is significantly greater than in a standard 1.3-μm GaInNAs sample. Therefore, in order to grow material below the critical thickness for dislocation formation, strain compensating material was grown surrounding the compressively strained QWs. Tensile strained GaNAs barriers 20 nm thick were used to prevent relaxation and permitted the growth of dislocation-free films thicker than 10 nm. Fig. 4 shows the

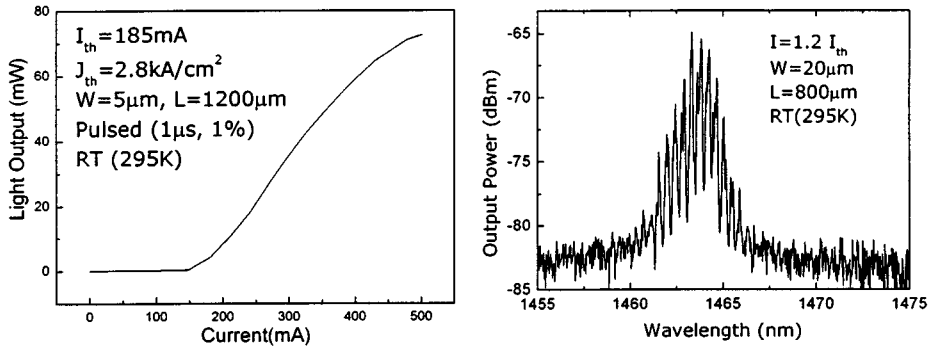

Fig. 5. L–I curve and optical spectrum for a GaInNAsSb–GaNAsSb ridge waveguide laser with peak emission at 1.465 μm. The In mole fraction is 44% and Sb flux was 6.86×10^{-8} torr.

(004) HRXRD pattern of GaInNAsSb and GaInNAs QW samples. Both samples were three highly compressive QWs 7 nm thick surrounded by 20-nm tensile barriers. The GaInNAsSb QW sample contained 37% In, 1.2% N, and 7.1×10^{-8} torr of Sb while the GaInNAs contained 30% In, and 1.2% N. The broad enveloped peak at small angles from the GaAs substrate corresponds to the (004) diffraction from the strained QW and represents 3.6% and 4.84% QW strain normal to the substrate for GaInNAs and GaInNAsSb, respectively. The increase in compressive strain of the QWs comes from both the increase of In composition and the addition of Sb. This additional strain would further limit the amount of gain medium available, further necessitating the use of tensile strain compensation in the barrier layers.

Other advantages exist for the use of GaNAs barrier material in active region designs. One factor for the blue-shift present during postgrowth anneal was found to be nitrogen out-diffusion from the QW. Both SIMS and HRXRD have observed this behavior from nitride-arsenide-based alloys. By surrounding the QWs with nitrogen containing material, the bandgap shift may be reduced due to less nitrogen loss [9], [10]. The active region design is actually simplified due to the fact that nitrogen incorporation in MBE is known to be unity sticking; therefore, it is inversely proportional to the group III growth rate. In the barrier, without the presence of In flux, the nitrogen concentration is higher than in the wells. Therefore, nitrogen in the barrier will be able to diffuse into the QW, reducing the amount lost. The amount of nitrogen lost from the barriers during anneal as seen in Fig. 2 is 10% while in the QWs the nitrogen content is reduced by only 8%. Another effect of nitride-containing barriers is the reduced confinement energy for carriers in the QWs. Carriers are still well confined by GaAs, which makes up the rest of the active region, but the confinement energy in the QW is reduced, allowing optical emission at lower energies.

It is not yet clear the effect Sb has on the optical properties of GaInNAs and the origin of the large PL peak shift. Simply attributing Sb with surfactant properties, which prevents three-dimensional (3-D) surface morphology during growth, may explain the improvement in luminescent intensity but not the large shift of emission wavelengths. However, there may be several explanations of the effect of Sb on GaInNAs using its possible surfactant like properties. It is also possible that the surface energy during growth has been modified such that there is enhanced nitrogen incorporation, further red-shifting output. However, both SIMS and RBS only measured slight increases in N composition with Sb, less than what is needed to explain this effect. Another explanation could be that Sb reduces phase segregation or potential fluctuations known to be present in GaInNAs [11]. In the GaInNAsSb alloy, an alternative mechanism for room-temperature radiative recombination may occur and carriers may recombine lower in the conduction band, reducing luminescent energies.

Other explanations are possible that do not consider antimony's role as a surfactant in GaInNAs. One factor could be increased confinement of holes in QW structures due to a larger valence band offset with increasing Sb. The addition of nitrogen is thought to mostly effect the conduction band offset caused by an interaction between the condition band and a localized N resonant state [12], [13]. With an improvement of hole confinement, PL efficiency may improve with more carriers captured in the QWs. It might also be possible that as the In concentration increases, the effective bandgap reduction of added N is decreased. However, small amounts of Sb may also reduce the bandgap but not reduce nitrogen's role in bandgap reduction. A final possible explanation is that Sb may increase the bowing of N in GaInAs [14], allowing small changes of Sb to greatly affect the bandgap. However, more work needs to be done to understand the role of Sb on luminescence in GaInNAs and find evidence that supports these speculative explanations.

Based on our PL study, multiple QW in-plane laser structures were grown on (100) n-GaAs substrate. The active region consisted of three 7-nm GaInNAs(Sb) QWs separated by 20-nm GaNAs(Sb) barriers. The active region was symmetrically embedded between 120-nm undoped GaAs waveguides. A 1.8-μm Si doped (5×10^{18} cm^{-3}) n-type bottom cladding layer was grown below the active region with a 1.7-μm Be doped (2×10^{18} cm^{-3}) p-type top cladding. A 50-nm (1×10^{19} cm^{-3}) GaAs cap layer was grown for metallization. The samples were then postgrowth annealed at 720 °C for 2 min by RTA. All lasers were operated under pulsed conditions of 1 μs with a 1% duty cycle. The first 1.32-μm laser with 3 $Ga_{0.68}In_{0.32}N_{0.015}As_{0.985}$ QWs and $GaAs_{0.98}N_{0.02}$ barriers had a threshold current density of 1.5 kA/cm^2 and a slope efficiency of 0.45 W/A (48%, from both facets) for a 770-μm-long by 20-μm-wide mesa. The maximum output power without device failure was 320 mW (from both facets) and operated up to 95 °C. To achieve longer laser

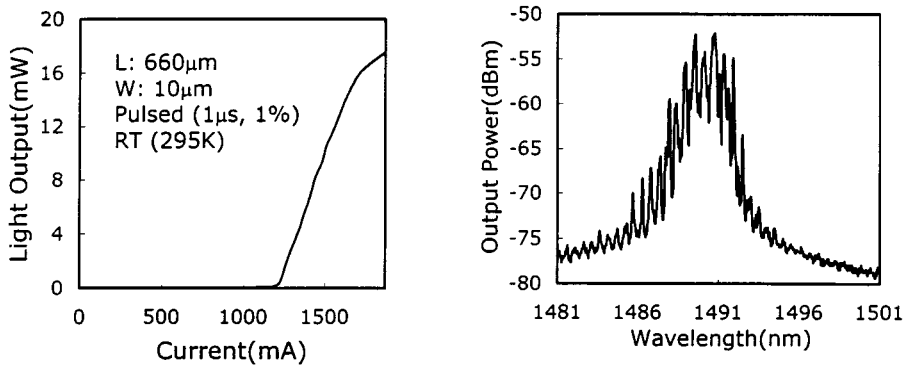

Fig. 6. L–I curve and optical spectrum for a GaInNAsSb–GaNAsSb ridge waveguide laser with peak emission at 1.49 μm. The indium mole fraction is 46% and Sb flux was 1.4×10^{-7} torr.

emission, a device with 3 $Ga_{0.65}In_{0.35}N_{0.017}As_{0.983}$ QWs and $GaAs_{0.978}N_{0.022}$ barriers was grown. This in-plane laser exhibited room-temperature operation out to 1.39 μm with a threshold current density of 1.8 kA/cm^2. The slope efficiency was 0.67 W/A (from both facets) above threshold current. The maximum output power was 350 mW from both facets without a heat sink or AR/HR coating. This maximum output power was achievable without device failure with a maximum operating temperature of 70 °C with no heat sink.

In order to obtain laser emission beyond 1.4 μm, it is necessary to incorporate more than 40% In to the GaInNAs QWs. This, however, is not easily achieved in MBE growth due to the lattice mismatch between GaAs and InAs and the solubility limit of N in GaAs. Alternatively, more nitrogen may be added but increased nitrogen-related defects cause much higher laser threshold currents [6]. Given the encouraging PL results with GaInNAsSb shown above, we introduced Sb during the active layer growth and were able to incorporate up to 46% In without lattice relaxation or the onset 3-D growth morphology. Based on our PL study, ridge waveguide lasers with three $Ga_{0.55}In_{0.45}N_{0.017}As_{0.953}Sb_{0.03}$ QWs and $GaN_{0.02}As_{0.9}Sb_{0.08}$ barriers were grown and fabricated. Fig. 5 shows the L–I curve and spectrum of a 5-μm-wide and 1200-μm-long stripe device at 1.465 μm with a maximum power exceeding 70 mW from both facets without device failure. The minimum threshold current density was 2.8 kA/cm^2 or 930 A/cm^2 per QW. To our knowledge, this is the lowest threshold current density for lasers with GaInNAs QWs beyond 1.4 μm on a GaAs substrate. A second in-plane laser with $Ga_{0.54}In_{0.46}N_{0.017}AsSb$ QWs, $GaN_{0.02}AsSb$ barriers and 1.4×10^{-7} torr Sb flux was fabricated and lased at 1.49 μm at room temperature (L-I and spectrum shown in Fig. 6). Further details about these GaInNAsSb lasers can be found in [15]. Lasers with emission at 1.55 μm and superior performance should be possible with further optimization of the In, N, and Sb compositions, growth temperature and annealing conditions.

IV. Conclusion

High-intensity PL was observed for dilute nitride GaInNAsSb structures from 1.3–1.6 μm. Antimony incorporation, measured using various analytical techniques, was found to be significant (as high as 8%). In-plane lasers fabricated with this material showed low threshold lasing at 1.465 μm and lasing as long as 1.49 μm. With future generation laser structures and optimization of the active region, longer wavelengths and lower thresholds should be possible.

Acknowledgment

The authors would like to thank S. P. Smith, L. Wei, G. R. Mound, and P. Van Lierde of Charles Evans & Associates for their SIMS and RBS work, and V. Lordi and K. Volz at Stanford University for their help in characterization and microscopy.

References

[1] M. Kondow, K. Uomi, A. Niwa, T. Kitantai, S. Watahiki, and Y. Yazawa, "GaInNAs: A novel material for long-wavelength-range laser diodes with excellent high-temperature performance," *Jpn. J. Appl. Phys.*, vol. 35, pp. 1273–1275, Feb. 1996.

[2] A. F. Phillips, S. J. Sweeney, A. R. Adams, and P. J. A. Thijs, "The temperature dependence of 1.3 and 1.55 μm compressively strained InGaAs(P) MQW semiconductor lasers," *IEEE J. Select. Topics Quantum Electron.*, vol. 5, pp. 401–412, May-June 1999.

[3] C. W. Coldren, M. C. Larson, S. G. Spruytte, and J. S. Harris Jr., "1200 nm GaAs based vertical cavity lasers employing GaInNA's multiple quantum well active region," *Electron. Lett.*, vol. 36, pp. 951–952, May 2000.

[4] S. Sato, Y. Osawa, T. Saitoh, and I. Fujimura, "Room-temperature pulsed operation of 1.3 μm GaInNAs/GaAs laser diode," *Electron. Lett.*, vol. 33, pp. 1386–1387, July 1997.

[5] M. R. Gokhale, P. V. Studentkov, J. Wei, and S. R. Forrest, "Low-threshold current, high-efficiency 1.3 μm wavelength aluminum-free InGaAsN-based quantum-well lasers," *IEEE Photon. Technol. Lett.*, vol. 12, pp. 131–133, Feb. 2000.

[6] M. O. Fischer, M. Reinhardt, and A. Forchel, "Room-temperature operation of GaInAsN-GaAs laser diodes in the 1.5-μm range," *IEEE J. Select. Topics Quantum Electron.*, vol. 7, pp. 149–151, Mar. 2001.

[7] H. Shimizu, K. Kumada, S. Uchiyana, and A. Kasukawa, "High-performance CW 1.26 μm GaInNAsSb-SQW ridge lasers," *IEEE J. Select. Topics Quantum Electron.*, vol. 7, pp. 355–364, Mar. 2001.

[8] X. Yang, M. J. Jurkovic, J. B. Heroux, and W. I. Wang, "Molecular beam epitaxial growth of InGaAsN : Sb/GaAs quantum wells for long-wavelength semiconductor lasers," *Appl. Phys. Lett.*, vol. 75, pp. 178–180, July 12, 1999.

[9] S. G. Spruytte, M. C. Larson, W. Wampler, C. W. Coldren, H. E. Petersen, and J. S. Harris, "Nitrogen incorporation in group III-nitride-arsenide materials grown by elemental source molecular beam epitaxy," *J. Cryst. Growth*, vol. 227–228, pp. 506–515, July 2001.

[10] W. Ha, V. Gambin, M. Wistey, S. Bank, S. Kim, and J. S. Harris, "Multiple quantum well GaInNAs/GaNA's ridge-waveguide laser diodes operating out to 1.4 μm," *IEEE Photon. Technol. Lett.*, 2002, to be published.

[11] I. A. Buyanova, W. M. Chen, G. Pozina, J. P. Bergman, B. Monemar, H. P. Xin, and C. W. Tu, "Mechanism for low-temperature photoluminescence in GaNAs/GaAs structures grown by molecular-beam epitaxy," *Appl. Phys. Lett.*, vol. 75, pp. 501–503, July 26, 1999.
[12] W. Shan, W. Walukiewicz, J. W. Ager III, E. E. Haller, J. F. Geisz, D. J. Friedman, J. M. Olson, and S. R. Kurtz, "Band anticrossing in GaInNA's alloys," *Phys. Rev. Lett.*, vol. 82, pp. 1221–1224, Feb. 9, 1999.
[13] J. D. Perkins, A. Maxcarenhas, Y. Zhang, J. F. Geisz, D. J. Friedman, J. M. Olson, and S. R. Kurtz, "Nitrogen-activated transitions, level repulsion, and band gap reduction in $GaAs_{1-x}N_x$ with $x < 0.03$," *Phys. Rev. Lett.*, vol. 82, pp. 3312–3315, Apr. 19, 1999.
[14] S. Wei and A. Zunger, "Giant and composition-dependent optical bowing coefficient in GaAsN alloys," *Phys. Rev. Lett.*, vol. 76, pp. 664–667, Jan. 22, 1996.
[15] W. Ha, V. Gambin, M. Wistey, S. Bank, H. Yuen, S. Kim, and J. S. Harris, "Long wavelength GaInNAsSb/GaNAsSb multiple quantum well lasers," *Electron. Lett.*, vol. 38, pp. 277–278, Mar. 2002.

Vincent Gambin received the M.S. degree in material science from Stanford University, Stanford, CA, in 2000 and the B.S. degree in ceramic engineering from Rutgers University, New Brunswick, NJ, in 1997. He is currently pursuing the Ph.D. degree in material science at Stanford, where he is studying the dilute nitride GaAs system for applications in long-wavelength optoelectronic devices.

Wonill Ha received the M.S. degree in electrical engineering from Stanford University, Stanford, CA, in 1998 and the B.S. degree in electronics engineering from Korea University, Seoul, Korea, in 1995. He is currently pursuing the Ph.D. degree in electrical engineering.

His research interests are high-power and long-wavelength lasers on GaAs.

Mark Wistey was born in Hillsboro, OR, on March 21, 1971. He received the M.S.E.E. degree from Stanford University, Stanford, CA, in 1999 and the B.S.E.E. degree from Montana State University-Bozeman in 1994. He is currently working on high-speed and long-wavelength VCSELs as a Ph.D. candidate at Stanford University.

Homan Yuen received the B.A. degree in physics (with an emphasis in solid state) from the University of California at Berkeley in 2000. He is currently working toward the Ph.D. degree in materials science and engineering at Stanford University and is studying the dilute nitride GaAs system for applications in long-wavelength optoelectronic devices.

Seth R. Bank received the B.S. degree in electrical engineering from the University of Illinois, Urbana-Champaign (UIUC), in 1999. While at UIUC, he worked on InGaP–GaAs and InGaAs–InP HBTs.

He is currently a Research Assistant at Stanford University, Stanford, CA, where he focuses on MBE growth and fabrication of long-wavelength VCSELs in the GaInNAsSb–GaAs material system.

Seongsin M. Kim received the B.S. degree in physics from Yonsei University, Seoul, Korea, in 1992, and the M.S. degree in physics in 1994 and the Ph.D. degree in electrical and computer engineering in 1999, both from Northwestern University, Evanston, IL. Her thesis work included MOCVD growth of self-assembled quantum dots and research on quantum dot lasers and detectors.

She is currently a Research and Development Engineer at Agilent Technologies Inc., where she works for developing high-bandwidth VCSELs for optical fiber data communication and device design of reliable long-wavelength VCSELs. She has been a consulting Assistant Professor in electrical engineering at Stanford University, Stanford, CA, since 2002. Her research interests include exploring new materials such as InGaAsN(Sb), high power laser application, and nanotechnology for photonic integrated circuits.

James S. Harris, Jr. (S'66–M'68–SM'77–F'88) received the B.S., M.S., and Ph.D. degrees in electrical engineering from Stanford University, Stanford, CA, in 1964, 1965, and 1969, respectively.

He is the James and Ellenor Chesebrough Professor of Engineering at the Electronics Laboratory of Stanford University. In 1969, he joined the Rockwell International Science Center, Thousand Oaks, CA, where he was one of the key contributors in developing their preeminent position in GaAs device technology. In 1982, he joined the Solid State Electronics Laboratory, Stanford University, as Professor of Electrical Engineering. He served as Director of the Solid State Electronics Laboratory at Stanford University from 1981 to 1988. His research interests are in the physics and application of ultrasmall structures to new electronic and optoelectronic devices and high-speed integrated circuits and MBE growth. He has more than 500 publications in these areas.

Dr. Harris received the Heinrich Walker medal, the IEEE Third Millennium Medal, and the 2000 IEEE Morris N. Liebmann Memorial Award for his contributions to GaAs devices and technology. He is a Fellow of the American Physical Society.